

Mobility theory of intermediate-bandwidth carriers in organic crystals: Scattering by acoustic and optical phonons

L. Giuggioli,¹ John D. Andersen,² and V. M. Kenkre¹

¹Center for Advanced Studies and Department of Physics and Astronomy, University of New Mexico, Albuquerque, New Mexico 87131

²Department of Physics, Rochester Institute of Technology, Rochester, New York 14623

(Received 15 August 2002; published 30 January 2003; publisher error corrected 18 March 2003)

An intermediate-bandwidth theory of charge-carrier mobility is developed with a focus on finite-band effects and scattering by phonons. Wide-band behavior is recovered as a limit. Two applications of the finite-band theory are discussed: in one a dip is predicted in the temperature dependence of the mobility, and in the other recently reported observations on ultrapure organic crystals are addressed.

DOI: 10.1103/PhysRevB.67.045110

PACS number(s): 72.80.Le, 72.10.-d, 72.20.-i, 72.20.Fr

I. INTRODUCTION AND BASIC EXPRESSIONS

Charge-carrier transport in inorganic crystals, e.g., metals such as Cu and semiconductors such as Ge, is described by textbook band theory.^{1,2} Carrier transport in organic crystals (such as naphthalene and pentacene) has been described in terms of polaronic theories with band effects either neglected or relegated to a secondary role.³⁻⁶ There is a need for an intermediate-bandwidth treatment in which band features are an essential starting ingredient of the theory, and in which the wide-band behavior seen in inorganic materials may be recovered in an appropriate limit. An approach toward the construction of such an intermediate bandwidth treatment was recently constructed by one of the present authors⁷ through elementary considerations of impurity scattering. The purpose of the present paper is to extend that approach to the more complex and realistic case of scattering by phonons, both acoustic and optical.

The paper is organized as follows. In the rest of Sec. I we display our starting point for the density of states, effective mass, and carrier velocity. The basic expressions for the acoustic and optical phonon scattering rates are studied in Sec. II. With a combination of these, carrier mobility expressions are obtained and discussed in Sec. III, where the more standard wide-band limit is recovered as a limiting case. Two applications of our theory constitute Sec. IV: the first discusses a curious dip in the mobility which we predict on the basis of our analysis, while the second addresses the temperature dependence of the mobility reported recently in experiment. Remarks form Sec. V.

Following Ref. 7 we assume an isotropical three-dimensional system and a single truncated parabolic band in our treatment. The assumption of a single band means that the band gap is large enough to make interband transitions unimportant. The choice of a free-electronic dispersion allows the treatment to yield the broadband limit smoothly.

A simple way to consider the finiteness of the bandwidth B is to take the density of states ρ corresponding to a parabolic band structure, i.e., with a $\sqrt{\varepsilon_k}$ dependence where ε_k is the carrier energy and k is the quasimomentum, and to vanish beyond the band edge:

$$\rho(\varepsilon_k) = \begin{cases} N \frac{3\sqrt{\varepsilon_k}}{2B^{3/2}}, & \varepsilon_k \leq B \\ 0, & \varepsilon_k > B. \end{cases} \quad (1)$$

N is the total number of atoms/molecules, and the specific B dependence is dictated simply by normalization of $\rho(\varepsilon_k)$. Considering a cubic lattice with lattice constant a , and expressing $N = N_c V/a^3$, where V is the volume and N_c is the number of atoms/molecules per unit cell, Eq. (1) can be integrated over all possible energy states and momentum states to find the maximum allowed k -vector in the band: $k_{\max} = (3\pi^2 N_c)^{1/3}/a$. Evaluating the parabolic band dispersion relation at k_{\max} , a direct relation between the effective mass m^* and B can be written:

$$m^* = \frac{\hbar^2 (3\pi^2 N_c)^{2/3}}{2a^2} \frac{1}{B}. \quad (2)$$

Using Eq. (2) we can write explicitly the energy dispersion relation as well as the speed of a carrier $v_k = \hbar^{-1} (d\varepsilon_k/dk)$ in the band as function of B :

$$\varepsilon_k = \frac{a^2 B}{(3\pi^2 N_c)^{2/3}} k^2, \quad (3)$$

$$v_k = \frac{2}{\hbar \sqrt{3}} \frac{a \sqrt{B \varepsilon_k}}{(3\pi^2 N_c)^{1/3}}. \quad (4)$$

Eqs. (1)–(4) are the starting point of the theory.

In keeping with general practice in the field, we will assume the Hamiltonian given by

$$H = \sum_k \varepsilon_k a_k^+ a_k + \sum_{\alpha, q} \hbar \omega_\alpha(q) \left(b_{q\alpha}^+ b_{q\alpha} + \frac{1}{2} \right) + H_{int} \quad (5)$$

where the first term describes the carrier, the second term represents acoustic ($\alpha = ac$) and/or optical ($\alpha = op$) phonons, and the carrier-phonon interaction is given by

$$H_{int} = N^{-1/2} \sum_{k, q, \alpha} [\hbar \omega_\alpha(q) g_\alpha(q) a_{k+q}^+ a_k b_{q\alpha} + \text{H.c.}], \quad (6)$$

ω_α and g_α being the phonon frequency and the dimensionless coupling constant, respectively.

II. SCATTERING RATES

We start with the standard time-dependent perturbation theory expression for the rate of scattering of a \vec{k} state by absorption and emission of one acoustic phonon of momentum \vec{q} ,

$$\frac{1}{\tau} = \frac{2\pi}{\hbar} \sum_{q,\alpha} \{ |\langle \vec{k} + \vec{q}, n_{q,\alpha} - 1 | H_{int} | \vec{k}, n_{q,\alpha} \rangle|^2 \delta(\varepsilon_{\vec{k} + \vec{q}, n_{q,\alpha} - 1} - \varepsilon_{\vec{k}, n_q} + \delta(\varepsilon_{\vec{k} - \vec{q}, n_{q,\alpha} + 1} - \varepsilon_{\vec{k}, n_{q,\alpha}}) | \langle \vec{k} - \vec{q}, n_{q,\alpha} + 1 | H_{int} | \vec{k}, n_{q,\alpha} \rangle|^2 \}, \quad (7)$$

where $n_{q,\alpha}$ stands for the thermal average (Bose-Einstein) of the number of phonons with wave vector q . Under the assumption of linear (Debye) dispersion for acoustic phonons, and through the use of Eq. (3), energy and momentum conservation for absorption or emission of one phonon yield

$$\varepsilon_{\vec{k} \pm \vec{q}, n_{q,\alpha} \mp 1} - \varepsilon_{\vec{k}, n_{q,\alpha}} = \frac{a^2 B}{(3\pi^2 N_c)^{2/3}} (q^2 \pm 2\vec{k} \cdot \vec{q}) \mp \hbar \omega(q), \quad (8)$$

where $\omega(q) = v_s q$, with v_s the speed of sound for acoustic phonons while $\omega(q) = \omega_0$ for optical phonons.⁸

A. Acoustic scattering rate

With the definitions

$$a_{\pm}(x) = 2 \left(\frac{3}{2\eta} \right)^{1/3} [\chi \pm \sqrt{x}], \quad (9)$$

$$g_{\pm}(y) = \frac{y^2 e^{(\pm \beta \hbar \omega_D y/2)}}{2 \sinh(\beta \hbar \omega_D y/2)}, \quad (10)$$

wherein $x = \varepsilon_k/B$, η is a geometrical factor ($\eta < 3$) explained in the Appendix, $\chi = (\hbar \omega_D/2B)(3/2\eta)^{1/3}$, ω_D is the Debye frequency, $\beta = 1/k_B T$ with k_B the Boltzmann constant, and y is a dimensionless phonon momentum; on the basis of Eqs. (7) and (8), calculations detailed in the Appendix give, for the scattering rate due to acoustic phonons,

$$\frac{1}{\tau_{ac}}(x) = \frac{3\pi}{4\hbar} \frac{(g_D \hbar \omega_D)^2}{B} f_{ac}(x). \quad (11)$$

Here g_D is the dimensionless coupling constant representative of acoustic scattering via the deformation potential treatment¹ and the function $f_{ac}(x)$ is defined separately depending on the range of values of $\hbar \omega_D/B$. For $\hbar \omega_D/B < 1/2(2\eta/3)^{1/3}$,

$$f_{ac}(x) = \frac{1}{\sqrt{x}} \begin{cases} \int_{a_-(x)}^{a_+(x)} dy g_-(y), & 0 \leq x < \chi^2 \\ \int_0^{a_+(x)} dy g_-(y) + \int_0^{xB/(\hbar \omega_D)} dy g_+(y), & \chi^2 \leq x < 4\chi^2 \\ \int_0^{a_+(x)} dy g_-(y) + \int_0^{-a_-(x)} dy g_+(y), & 4\chi^2 \leq x < (1-2\chi)^2 \\ \int_0^{(1-x)B/(\hbar \omega_D)} dy g_-(y) + \int_0^{-a_-(x)} dy g_+(y), & (1-2\chi)^2 \leq x \leq 1; \end{cases} \quad (12)$$

for $1/2(2\eta/3)^{1/3} \leq \hbar \omega_D/B < (2/3)(2\eta/3)^{1/3}$,

$$f_{ac}(x) = \frac{1}{\sqrt{x}} \begin{cases} \int_{a_-(x)}^{a_+(x)} dy g_-(y), & 0 \leq x < \chi^2 \\ \int_0^{a_+(x)} dy g_-(y) + \int_0^{xB/(\hbar \omega_D)} dy g_+(y), & \chi^2 \leq x < (1-2\chi)^2 \\ \int_0^{(1-x)B/(\hbar \omega_D)} dy g_-(y) + \int_0^{xB/(\hbar \omega_D)} dy g_+(y), & (1-2\chi)^2 \leq x < 4\chi^2 \\ \int_0^{(1-x)B/(\hbar \omega_D)} dy g_-(y) + \int_0^{-a_-(x)} dy g_+(y), & 4\chi^2 \leq x \leq 1; \end{cases} \quad (13)$$

for $(2/3)(2\eta/3)^{1/3} \leq \hbar \omega_D/B < (2\eta/3)^{1/3}$,

$$f_{ac}(x) = \frac{1}{\sqrt{x}} \begin{cases} \int_{a_-(x)}^{a_+(x)} dy g_-(y), & 0 \leq x < (1-2\chi)^2 \\ \int_{a_-(x)}^{(1-x)B/(\hbar\omega_D)} dy g_-(y), & (1-2\chi)^2 \leq x < \chi^2 \\ \int_0^{(1-x)B/(\hbar\omega_D)} dy g_-(y) + \int_0^{xB/(\hbar\omega_D)} dy g_+(y), & \chi^2 \leq x < 4\chi^2 \\ \int_0^{(1-x)B/(\hbar\omega_D)} dy g_-(y) + \int_0^{-a_-(x)} dy g_+(y), & 4\chi^2 \leq x \leq 1; \end{cases} \quad (14)$$

and, for $(2\eta/3)^{1/3} \leq \hbar\omega_D/B \leq 2(2\eta/3)^{1/3}$,

$$f_{ac}(x) = \frac{1}{\sqrt{x}} \begin{cases} 0, & 0 \leq x < (2\chi-1)^2 \\ \int_{a_-(x)}^{(1-x)B/(\hbar\omega_D)} dy g_-(y), & (2\chi-1)^2 \leq x < \chi^2 \\ \int_0^{(1-x)B/(\hbar\omega_D)} dy g_-(y) + \int_0^{xB/(\hbar\omega_D)} dy g_+(y), & \chi^2 \leq x \leq 1. \end{cases} \quad (15)$$

Note that for $\hbar\omega_D/B > 2(2\eta/3)^{1/3}$, $f_{ac}(x) = 0$ independently of the temperature.

The need for separate expressions for the various regimes for $f_{ac}(x)$ is a consequence of the introduction of a cutoff in the density of states which stems from the finiteness of the band. In the limit $\hbar\omega_D/B \rightarrow 0$, i.e., $\chi \rightarrow 0$, the cutoff disappears and only one regime survives in $f_{ac}(x)$: the one represented by the third expression in Eq. (12) with $a_+(x) = -a_-(x) = 2(3/2\eta)^{1/3}\sqrt{x}$. Clearly, $\tau_{ac}^{-1}(x)$ decreases down to zero as the ratio $\hbar\omega_D/B$ becomes larger since the constraints of energy and momentum conservation cannot be satisfied simultaneously.⁹

B. Optical scattering rate

For optical phonons, the counterpart of Eq. (11), as detailed in the Appendix, is

$$\frac{1}{\tau_{op}}(x) = \frac{3\pi}{4\hbar} \frac{(g_0\hbar\omega_0)^2}{B} f_{op}(x). \quad (16)$$

Here g_0 , the dimensionless coupling constant to optical phonons, ω_0 , the optical phonon frequency, and $f_{op}(x)$ take the respective places of g_D , ω_D , and $f_{ac}(x)$ in Eq. (11).

The function $f_{op}(x)$ is defined, as in the acoustic case, depending on the range of values of $\hbar\omega_0/B$. For $\hbar\omega_0/B < 1/2$,

$$f_{op}(x) = \begin{cases} \frac{e^{-\beta\hbar\omega_0/2}}{\sinh(\beta\hbar\omega_0/2)} \sqrt{x + \frac{\hbar\omega_0}{B}}, & 0 \leq x \leq \frac{\hbar\omega_0}{B} \\ \frac{e^{-\beta\hbar\omega_0/2} \sqrt{x + \frac{\hbar\omega_0}{B}} + e^{\beta\hbar\omega_0/2} \sqrt{x - \frac{\hbar\omega_0}{B}}}{\sinh(\beta\hbar\omega_0/2)}, & \frac{\hbar\omega_0}{B} < x < 1 - \frac{\hbar\omega_0}{B} \\ \frac{e^{\beta\hbar\omega_0/2}}{\sinh(\beta\hbar\omega_0/2)} \sqrt{x - \frac{\hbar\omega_0}{B}}, & 1 - \frac{\hbar\omega_0}{B} \leq x \leq 1; \end{cases} \quad (17)$$

while, for $1/2 \leq \hbar\omega_0/B \leq 1$,

$$f_{op}(x) = \begin{cases} \frac{e^{-\beta\hbar\omega_0/2}}{\sinh(\beta\hbar\omega_0/2)} \sqrt{x + \frac{\hbar\omega_0}{B}}, & 0 \leq x \leq 1 - \frac{\hbar\omega_0}{B} \\ 0, & 1 - \frac{\hbar\omega_0}{B} < x < \frac{\hbar\omega_0}{B} \\ \frac{e^{\beta\hbar\omega_0/2}}{\sinh(\beta\hbar\omega_0/2)} \sqrt{x - \frac{\hbar\omega_0}{B}}, & \frac{\hbar\omega_0}{B} \leq x \leq 1; \end{cases} \quad (18)$$

and $f_{op} = 0$ when $\hbar\omega_0/B > 1$. In the limit $\hbar\omega_0/B \rightarrow 0$ it is easy to see that the only terms which survive in $\tau_{op}^{-1}(x)$ are the first two expressions in Eq. (17).

Similarly to the acoustic case, $\tau_{op}^{-1}(x)$ becomes smaller as the ratio $\hbar\omega_0/B$ becomes larger and eventually vanishes. On the other hand, *differently* from acoustic scattering, a non-negligible change in the energy of the carrier is always involved in an optical scattering event. This is an important aspect, as we will see in Sec. IV. Indeed under certain conditions, it can give rise to a nonmonotonic temperature behavior of the mobility, a regime which is absent in the wide-band theory.

III. MOBILITY

Following a standard Boltzmann equation treatment, but making a finite-bandwidth modification as in Ref. 7, the mobility can be written as

$$\mu = q\beta \langle v_k^2 \tau_k \rangle = q\beta \frac{\int_0^B d\varepsilon_k \rho(\varepsilon_k) v_k^2 \tau(\varepsilon_k) e^{-\beta\varepsilon_k}}{\int_0^B d\varepsilon_k \rho(\varepsilon_k) e^{-\beta\varepsilon_k}}. \quad (19)$$

$$\mu = \frac{qa^2}{\hbar} \frac{2^4}{3^{8/3} N_c^{2/3} \pi^{7/3}} (B\beta)^{5/2} [\gamma(3/2, B\beta)]^{-1} \int_0^B d\varepsilon_k \frac{\varepsilon_k^{3/2} e^{-\varepsilon_k\beta}}{\frac{4\hbar\alpha_{imp}B^{3/2}}{3\pi} + g_D^2(\hbar\omega_D)^2 \sqrt{B} f_{ac}\left(\frac{\varepsilon_k}{B}\right) + g_0^2(\hbar\omega_0)^2 \sqrt{B} f_{op}\left(\frac{\varepsilon_k}{B}\right)}, \quad (21)$$

where γ is the incomplete gamma function.

Equations (19)–(21), which are the central result of our paper, contain effects of finiteness of the band. We now show how to recover from that result the well-known wide-band expression for μ .

The wide-band result, as commonly displayed without the impurity scattering term, is¹

$$\mu_\infty = \frac{2^{5/2} N_c \sqrt{\pi} q \hbar^4}{3a^3} \left(\frac{\beta}{m^*} \right)^{5/2} \times \int_0^\infty d\varepsilon_k \frac{\varepsilon_k^{3/2} e^{-\varepsilon_k\beta}}{g_D^2(\hbar\omega_D)^2 F_{ac}(\varepsilon_k) + g_0^2(\hbar\omega_0)^2 F_{op}(\varepsilon_k)}, \quad (22)$$

wherein

$$F_{ac} = \frac{B}{s^3 \sqrt{\varepsilon_k}} \int_0^{2s\sqrt{\varepsilon_k/B}} dq q^2 \coth(\beta\hbar v_s q/2) \quad (23)$$

with $s = (2\pi^2 \eta N_c)^{1/3}/a$, and

$$F_{op} = \frac{2}{e^{\beta\hbar\omega_0} - 1} [\sqrt{\varepsilon_k + \hbar\omega_0} + e^{\beta\hbar\omega_0} \Theta(\varepsilon_k - \hbar\omega_0) \sqrt{\varepsilon_k - \hbar\omega_0}], \quad (24)$$

The scattering sources we consider are acoustic phonons, optical phonons, and static impurities. From expressions we have derived above [Eqs. (11)–(16)] for the first two of these, we write, for $\tau(\varepsilon_k)$ due to all three sources,

$$\tau(\varepsilon_k) = \frac{4\hbar(3\pi B)^{-1}}{\frac{4\hbar\alpha_{imp}}{3\pi B} + \frac{(g_D\hbar\omega_D)^2}{B^2} f_{ac}\left(\frac{\varepsilon_k}{B}\right) + \frac{(g_0\hbar\omega_0)^2}{B^2} f_{op}\left(\frac{\varepsilon_k}{B}\right)}. \quad (20)$$

Here we have assumed for simplicity that the scattering rate due to impurities is constant (proportional to α_{imp} as, for instance, in Ref. 10, and have invoked Matthiessen's rule¹¹ that rates add). For a study of more general impurity scattering (k dependent, B dependent, etc.) we refer the reader elsewhere.¹² Using Eqs. (1), (4), and (20) we can write expression (19) for μ as

with Θ the Heaviside function. First we notice that if $\beta\hbar\omega_D \ll 1$, Eq. (23) reduces to its high- T limit $4\sqrt{\varepsilon_k}(\beta\hbar\omega_D)^{-1}$. Equation (22) in the high- T approximation for the acoustic scattering has been used successfully in the past¹ in the analysis of Si and Ge mobility data.

To recover the wide-band limit [Eq. (22)] from our Eq. (21), we first put $\alpha_{imp}=0$ in Eq. (21), and then notice that our f_{ac} and f_{op} functions yield the wide-band F_{ac} and F_{op} in the limits

$$\lim_{\hbar\omega_D/B \rightarrow 0} \sqrt{B} f_{ac}(\varepsilon_k/B) = F_{ac}(\varepsilon_k), \quad (25)$$

$$\lim_{\hbar\omega_0/B \rightarrow 0} \sqrt{B} f_{op}(\varepsilon_k/B) = F_{op}(\varepsilon_k). \quad (26)$$

Substituting in Eq. (21) the upper limits of integration B by ∞ , recognizing that the incomplete gamma function transforms into the (complete) gamma function $\Gamma(3/2)$, and expressing $B^{5/2}$ through Eq. (2) as function of m^* , we obtain the wide-band formula.

In order to understand the differences in the wide-band and intermediate-band results in the range of parameters for which the differences are not dramatic, we display Fig. 1, where Eqs. (21) and (22) are plotted. We take some representative values of the parameters as explained in the figure caption. It is seen that, as the ratio $\hbar\omega_{D,0}/B$ becomes larger, wide-band predictions become less accurate. Generally, finite-band μ has a steeper dependence than wide-band μ at

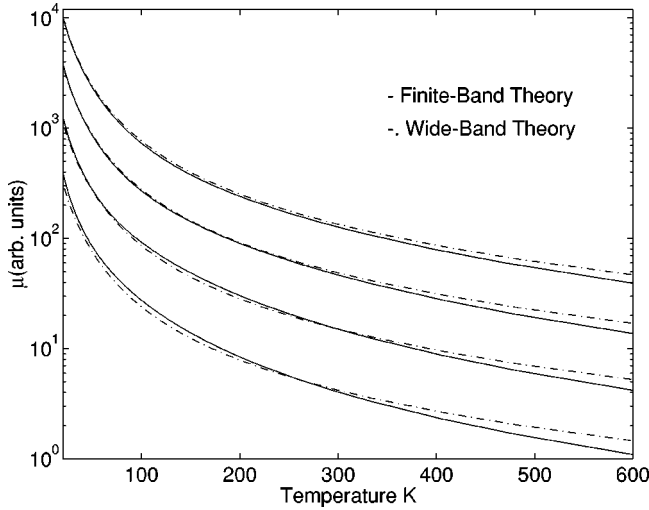


FIG. 1. Comparison between the mobility predictions of wide-band theory [Eq. (22)] and our finite-band theory [Eq. (21)]. From top to bottom, the values of $\hbar\omega_0/B$ are 1/6, 1/4, 2/5, and 2/3; $g_0 = 0.1$, $g_D = 0.3$, $\hbar\omega_D = 5$ meV, $\hbar\omega_0 = 15$ meV, $\hbar\alpha_{imp} = 0$, $\eta = 3/2$, and $N_c = 2$. Note that the larger the ratio $\hbar\omega_0/B$, the larger is the effect of the finiteness of B .

high T . This can be understood as arising from two opposite trends in the finite-band theory. On the one hand, the existence of a cutoff in the density of states for the carrier implies that scattering transitions involving final states outside the band are not allowed. This has the effect of increasing μ . On the other hand, lower values of B represent slower velocities and consequently lower μ . These combined effects make the T dependence of μ when $\beta\hbar\omega_{D,0} \ll 1$ different from the $T^{-1.5}$ typical for inorganic semiconductors.¹³

IV. APPLICATIONS

We apply our finite-band theory to two situations. In the first, we show that optical scattering can produce a curious dip in the mobility if B is small enough, specifically comparable to the optical-phonon energy. In the second, we analyze recently reported observations in ultrapure organic crystals.

A. Prediction of a dip in the mobility

Optical-phonon scattering possesses the characteristic that it requires a finite amount of energy interchange with the carrier. Therefore, if optical-phonon scattering predominates, and if the carrier bandwidth is comparable to the optical phonon energy, a remarkable effect can occur: a *rise* in the mobility as a function of T as shown in Fig. 2. Figure 2 shows both the occurrence of the phenomenon and how the rise, or equivalently the dip, tends to disappear if, as explained in the next paragraph, the region of forbidden optical transitions is too large (top curve) or too small (bottom curve). The flat part of the curves for T close to zero is due to impurity scattering. The sharp decrease at low T is an indication of the activation of optical phonon scattering. Between the value 0.1 and 0.5 of the normalized temperature, the three cases differ from one another substantially although

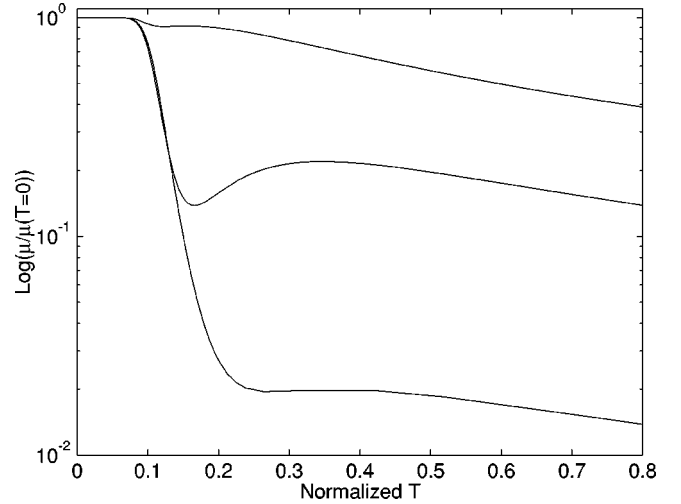


FIG. 2. Prediction of a dip and a rise in mobility, a finite-band effect. Shown are mobility curves normalized to the value at $T = 0$ versus $k_B T / \hbar\omega_0$ with $g_0 = 0.6$, $g_D = 0$ and $\alpha_{imp}/\omega_0 = 10^{-4}$ for different values of B . From top to bottom, $2\hbar\omega_0/B = 1.82$, 1.18, and 1.02, respectively.

$\hbar\omega_0/B$ differs only slightly. Beyond the value 0.5 of the normalized temperature, all three curves exhibit the same high- T behavior: a T^{-1} dependence characteristic of constant impurity scattering.⁷ This corresponds to the fact that $B < 2\hbar\omega_0$ for all three curves. If we take $B \geq 2\hbar\omega_0$, the T dependence (not shown in Fig. 2) becomes $T^{-2.5}$, as mentioned above.¹³ If the coupling to acoustic phonons or the amount of impurity scattering is increased, the dip tends to be masked, i.e., it disappears. For this reason we believe that the dip will not be observed in many realistic situations, unless the crystals are truly ultrapure.

If $B < 2\hbar\omega_0$, there is an energy region in the carrier band bounded from below by $B - \hbar\omega_0$ and limited above by $\hbar\omega_0$, where optical scattering is forbidden. In the bottom part of the band ($\varepsilon_k < B - \hbar\omega_0$), absorption of an optical phonon moves a carrier to the top part of the band, while emission of an optical phonon in the top part of the band ($\varepsilon_k > \hbar\omega_0$) moves a carrier to the bottom of the band. These are the only energetically allowed optical-phonon transitions.¹⁴

Since Eq. (19) shows that the expression for μ involves a thermal band average of the scattering time $\tau(\varepsilon_k)$, we display $\tau(\varepsilon_k)$ in Fig. 3 to clarify the origin of the dip. We have chosen arbitrary parameters as shown in the figure caption, but the range of the carrier energy is from 0 to the bandwidth B . As T is raised, regions of higher energy get more populated. For low enough T , the region of forbidden optical scattering is hardly occupied. The dip effect occurs once T is large enough to populate the forbidden region. Scattering is suppressed and the mobility increases. As T increases still further, the average occupation of the carrier goes beyond the forbidden region, scattering suppression is stopped, and μ decreases again. The majority of the carriers at low T see a scattering time $\tau(\varepsilon_k)$ as shown in the left part of Fig. 3. For higher T , the main mechanism of relaxation for the carrier distribution becomes impurity scattering: see the middle portion of Fig. 3. On increasing T further, the carriers have

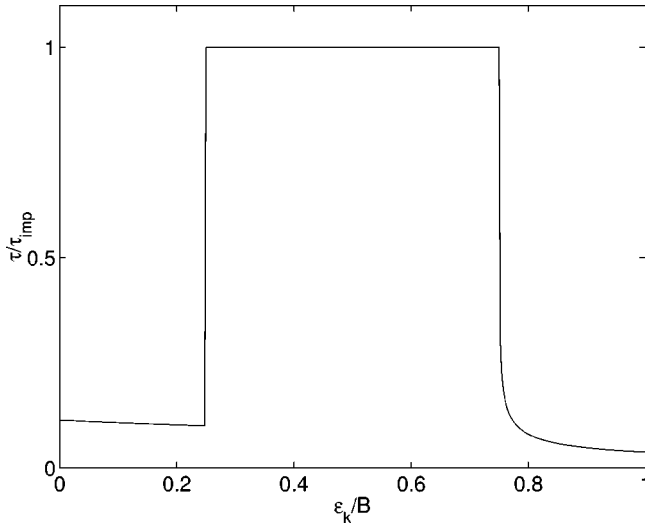


FIG. 3. Origin of the dip/rise effect. Shown is the optical scattering time normalized to the impurity value τ_{imp} as a function of the relative carrier energy in the band $x = \epsilon_k/B$ for the (arbitrary) parameters $g_0 = 0.6$, $g_D = 0$, $\beta\hbar\omega_0 = 3.5$, $\hbar\alpha_{imp}/B = 5.00 \times 10^{-5}$, and $\hbar\omega_0/B = 0.75$.

access also to regions in the band where $\tau(\epsilon_k)$ is given by the right portion of Fig. 3. Thus the resulting shape of the $\mu(T)$ curve reflects, more or less, the shape of the scattering time $\tau(\epsilon_k)$. As remarked upon earlier, this predicted dip may not be observed in many systems because of the existence of non-negligible scattering from sources other than optical phonons.¹⁵

B. Description of low- T data in pentacene

As a second application of our general mobility result [Eq. (21)], we address recently reported mobility data on pure pentacene crystals in the range 20–400 K. As in Ref. 16, we have chosen only a partial range of data which is

compatible with a band description.¹⁷ The chosen range is the one for which μ obeys a clear power law $\mu \sim T^{-2.7}$.

It is at once clear from wide-band theory that it is impossible to address these data if the sole scattering source is acoustic phonons since the latter lead to the well-known $T^{-1.5}$ law of μ in contrast to the observed $T^{-2.7}$ dependence. Similarly, it becomes clear on quantitative analysis, as in Ref. 16, that optical phonons alone cannot provide an explanation since they involve an uncomfortably steep decrease of μ at low T and a $T^{-1.5}$ behavior at high T . It is, however, possible to produce reasonable fits to the data by a combination of the two kinds of scattering by following a procedure used in an early analysis¹ of μ in the inorganic material Ge, but augmented through our finite-band expression.

We take as inputs ω_D and ω_0 . Outputs are the quality of the fit and the values of the coupling constants g_D and g_0 . Choosing $\hbar\omega_D = 8.3$ meV as a reasonable value smaller than the lowest optical frequency, we verify that it corresponds to a reasonable calculated speed of sound of 2.88×10^5 cm/sec which lies comfortably in the known range $(1-5) \times 10^5$ cm/sec. Smaller values of $\hbar\omega_D$ do not change appreciably either the quality of the fit or the values of the coupling constants. In keeping with known spectra of pentacene,¹⁸ we take ω_0 to be each of the spectrally known values (starting with 8.5 meV) in turn. We assume various values of B and perform a least-squares fit to the pentacene data. The fit quality improves for higher assumed optical frequencies. Optical frequencies higher than 15.5 meV are found to be unacceptable because the limiting B are even smaller than $\hbar\omega_0$, making optical scattering impossible. In Fig. 4 we display reported pentacene data in the 20–400 K range along with our fits. Resulting fits look acceptable on visual inspection.

The primary conclusion to be drawn from the fitting is provided by varying the assumed B and checking for internal consistency. This check is provided by the ratio of the mean free path λ to the lattice constant a , obtained by multiplying the velocity of the carrier by the scattering time in Eq. (20) and averaging over the band;

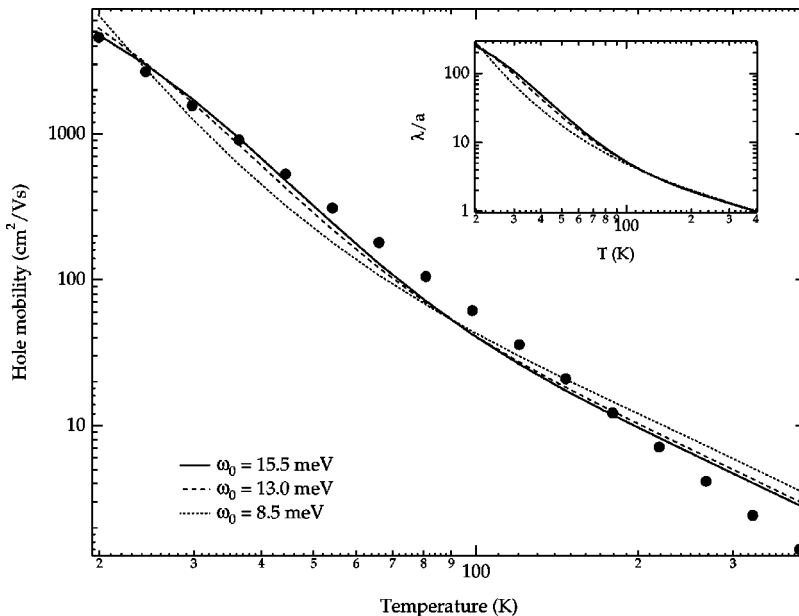


FIG. 4. Least-squares fits of Eq. (21) to reported pentacene data with several optical frequencies. Extracted parameters and the maximum allowed B are listed in Table I. The inset shows the ratio of the mean free path to the lattice constant for the corresponding fits.

TABLE I. Parameters extracted from the fit of Eq. (21) with the maximum allowed B . The corresponding mobility curves and ratios of the mean free path to the lattice constant are shown in Fig. 4.

Inputs		Limits	Outputs	
$\hbar\omega_D(\text{meV})$	$\hbar\omega_0(\text{meV})$	$B(\text{meV})$	g_D	g_0
8.3	8.5	49.4	0.08	0.56
8.3	13	39.6	0.13	0.40
8.3	15.5	36.7	0.13	0.36

$$\frac{\lambda}{a} = \frac{2^{2/3}}{3^{5/6}\pi^{2/3}} \frac{B}{\hbar} \frac{\int_0^1 dx x \tau(x) e^{-\beta x B}}{\int_0^1 dx \sqrt{x} e^{-\beta x B}}. \quad (27)$$

We plot λ/a as an inset in Fig. 4 after imposing the requirement on the calculational procedure that this ratio has the minimum allowable value of 1 at the extreme of the T range (400 K). This results in upper limits to B which are listed in Table I.

At first glance it might appear counterintuitive that the condition $\lambda/a > 1$ should lead to an upper rather than lower limit on B . Larger B , one might expect, leads to larger λ . However, these limits emerge from a fitting of the theory to (given) experimental values of μ which is essentially given by $\mu \sim v^2 \tau \sim v \lambda$, since $v \tau \sim \lambda$. Given the observed values of μ , the relationship $\lambda \sim \mu/v$ shows that larger λ require smaller v , i.e., smaller B . Such considerations have been given earlier^{16,19} on the basis of gross estimates for λ . We have made the criteria more stringent here, by calculating energy-dependent λ 's and taking their thermal average [see Eq. (27)].

Given that calculated²⁰ (and expected) values of the bare bandwidth in pentacene are larger than, or of the order of, 500 meV, in contrast to an order of magnitude smaller limit we have obtained through our fitting (see Table I), we can draw one of several conclusions: (i) that band theory is inapplicable in pentacene even in the context of the reported low- T data; (ii) that the calculated²⁰ and observationally²¹ expected values of B are incompatible with transport experiments; or (iii) that the B limit of 50 meV which arises from our fitting is not the true bare bandwidth but one already reduced by a Huang-Rhys (HR) factor stemming from strong interactions with a high intramolecular frequency vibration. The present authors tend to believe the current calculations²⁰ of B , and therefore to draw conclusion (iii). Indeed, we repeated the fitting procedure by replacing B by the HR expression $B = B_0 e^{-G^2 \coth(\hbar\Omega/2k_B T)}$, where Ω is the frequency of the intramolecular vibration with which the carrier is supposed to interact strongly. We found that for $\hbar\Omega > 120$ meV, the HR factor reduces B to $B_0 \exp(-G^2)$ at $T = 0$ and is essentially T independent in the 20–400-K range. In order to satisfy the condition $\lambda/a > 1$ with the assumed large $B_0 = 600$ meV,²⁰ the restraints on B require a value of $G \geq 1.6$.

V. REMARKS

The purpose of the present paper has been to develop an intermediate-band theory of the mobility of charge carriers scattered by phonons, starting from a standard Boltzmann equation approach but incorporating the finiteness of the bandwidth directly into the calculations. Such a theory, in the restricted context of energy-independent impurity scattering, has been given in a recent study.⁷ The present calculation extends the considerations of that study to realistic situations involving carrier scattering by acoustic and optical phonons as well as by impurities. The eventual aim of the theory is to join polaronic calculations which are current in narrow-band organic materials^{3,4} with broadband considerations which are common in wide-band inorganic materials.^{1,12}

Fermi Golden rule prescriptions such as Eq. (7) have led us to derive explicit (although rather complex) expressions [Eqs. (11)–(18)] for the scattering rates arising from acoustic and optical phonon scattering. With their help we have obtained the mobility in Eq. (21). The wide-band limit^{1,12} has been recovered explicitly in Eq. (22), thus making contact with earlier results.

Finite-band theory leads to two opposite trends in the mobility. On one hand, a cutoff in the density of states for the carrier reduces the number of allowed scattering transitions, leading to higher μ . On the other hand, reduced B values corresponds to reduced velocities and therefore to lower μ . A straightforward consequence of these competing effects is obvious from Fig. 1 where the temperature dependence of the mobility shows that the mobility can exceed the wide-band result in one range but be exceeded by it in another. A more interesting consequence is in the first of the two applications we have given: the predicted rise in the mobility provided $B < 2\hbar\omega_0$. Such a rise comes about when a carrier enters the energy region where optical phonon scattering is absent.

The other application we have presented is to the reported observations in pentacene. Fitting with our theory leads to the conclusion that the reported mobility data in the partial T range (20–400 K) can be explained with recently calculated²⁰ large bare bandwidth values (> 500 meV) only if the carrier strongly interacts with a high-frequency intramolecular vibration, reducing its effective bandwidth even at the lowest of accessible temperatures by a factor of an order of magnitude.

The most accurate calculations would take the actual density of states of the carriers complete with its van Hove singularity structure. Our use of a density of states corresponding to the truncated parabolic band is obviously an approximation but one which, we hope, addresses the essentials. It certainly has the advantage of simplicity. Moreover, it tends to the correct wide-band behavior in the limit of a large bandwidth. Such a limit is inaccessible to treatments³ which use Gaussian density of states.

The present calculation serves as a stepping stone to a full theory²² of the mobility of charge carriers in pure organic crystals in cases where the low temperature data cannot be explained via narrow-band polaronic theories such as in

Ref. 4 while high-temperature data do require a polaronic analysis.

ACKNOWLEDGMENT

This work was supported in part by the NSF under Grant No. DMR-0097204 and by the Los Alamos National Laboratory under a contract to the Consortium of the Americas for Interdisciplinary Science of the University of New Mexico. We thank Professor Paul E. Parris for helpful discussions.

APPENDIX

1. Acoustic scattering rate

In the deformation potential approach for acoustic scattering the matrix element of the Hamiltonian H_{int} can be written out explicitly¹ as a function of ω_D , g_D , v_s , a , N_c , and $n_{q,ac}$. Taking the direction of \vec{k} as the z axis and integrating over all possible momenta q , Eq. (7) becomes

$$\frac{1}{\tau_{ac}} = \frac{1}{\hbar(2\pi)^2} \int_{q_{\min}}^{q_{\max}} q^2 dq \int_0^{2\pi} d\phi \frac{g_D^2 \hbar \omega_D a^3}{N_c} \hbar v_s q \times [I_{ac}(\vec{k} + \vec{q}) n_{q,ac} + I_{ac}(\vec{k} - \vec{q})(n_{q,ac} + 1)], \quad (\text{A1})$$

where q_{\min} and q_{\max} simply indicates that the scattering rate is nonzero only for certain values of phonon momentum defined by the two following positive quantities:

$$I_{ac}(\vec{k} + \vec{q}) = \int_0^\pi \delta \left[\frac{a^2 B}{(3\pi^2 N_c)^{2/3}} (q^2 + 2kq \cos \theta) - \hbar v_s q \right] \Theta \left[B - \frac{a^2 B}{(3\pi^2 N_c)^{2/3}} (q^2 + 2kq \cos \theta + k^2) \right] \sin \theta d\theta \quad (\text{A2})$$

$$I_{ac}(\vec{k} - \vec{q}) = \int_0^{\arccos(\zeta)} \delta \left[\frac{a^2 B}{(3\pi^2 N_c)^{2/3}} (q^2 - 2kq \cos \theta) + \hbar v_s q \right] \Theta \left[\frac{a^2 B}{(3\pi^2 N_c)^{2/3}} (q^2 - 2kq \cos \theta + k^2) \right] \sin \theta d\theta. \quad (\text{A3})$$

The angle $\zeta = q(2k)^{-1} + \hbar v_s (3\pi^2 N_c)^{2/3} (2a^2 B k)^{-1} = q/2k + v_s/v_k$ comes from imposing the condition $q \geq 0$ on the expression in Eq. (8) corresponding to the emission process. $\zeta > 0$ implies that only forward emission is allowed, and $\zeta < 1$ implies that when $v_k < v_s$ no emission process is possible.¹² The cutoffs due to the presence of the Heaviside function Θ assure that the final momentum state of the carrier stays inside the band: this is a feature missing in the calculation of scattering rate in large-band inorganic semiconductors.

With the substitutions

$$x_{\pm} = \frac{a^2 B}{(3\pi^2 N_c)^{2/3}} (q^2 \pm 2kq \cos \theta) \mp \hbar v_s q, \quad dx_{\pm} = \mp \frac{a^2 B}{(3\pi^2 N_c)^{2/3}} 2kq \sin \theta d\theta, \quad (\text{A4})$$

Eqs. (A2) and (A3) become, respectively,

$$I_{ac}(\vec{k} + \vec{q}) = \frac{(3\pi^2 N_c)^{2/3}}{2a^2 B k q} \int_{\tilde{a}_1}^{\tilde{a}_0} dx_+ \delta(x_+) \times \Theta[B - (x_+ + \varepsilon_k + \hbar v_s q)] = \frac{(3\pi^2 N_c)^{2/3}}{2a^2 B k q} \left\{ \left[\Theta \left(q + 2k - \frac{(3\pi^2 N_c)^{2/3} \hbar v_s}{a^2 B} \right) - \Theta \left(q - 2k - \frac{(3\pi^2 N_c)^{2/3} \hbar v_s}{a^2 B} \right) \right] \times \Theta(B - \varepsilon_k - \hbar v_s q) \right\}, \quad (\text{A5})$$

$$I_{ac}(\vec{k} - \vec{q}) = \frac{(3\pi^2 N_c)^{2/3}}{2a^2 B k q} \int_{\tilde{e}_1}^0 dx_- \delta(x_-) \Theta[x_- + \varepsilon_k - \hbar v_s q] = \frac{(3\pi^2 N_c)^{2/3}}{2a^2 B k q} \times \left\{ \left[1 - \Theta \left(q - 2k + \frac{(3\pi^2 N_c)^{2/3} \hbar v_s}{a^2 B} \right) \right] \times \Theta(\varepsilon_k - \hbar v_s q) \right\}, \quad (\text{A6})$$

where

$$\tilde{a}_0 = a^2 B (3\pi^2 N_c)^{-2/3} (q^2 + 2kq) - \hbar v_s q,$$

$$\tilde{a}_1 = a^2 B (3\pi^2 N_c)^{-2/3} (q^2 - 2kq) - \hbar v_s q,$$

and

$$\tilde{e}_1 = a^2 B (3\pi^2 N_c)^{-2/3} (q^2 - 2kq) + \hbar v_s q.$$

In order to rescale the above expressions appropriately, it is necessary to express v_s in terms of ω_D . Assuming the speed of sound identical for the longitudinal and the transverse modes, the Debye frequency ω_D can be related to v_s in the usual way through the relation

$$\omega_D = v_s (2\pi^2)^{1/3} \left(\frac{\eta N}{V} \right)^{1/3} = v_s (2\pi^2)^{1/3} \left(\frac{\eta N_c}{a^3} \right)^{1/3}, \quad (\text{A7})$$

where ηN represents the total number of acoustic modes, the value of η depending on the geometrical configuration of the crystal. For example, for a spherical molecule there are a

total of $3N$ available modes (no rotation): if $N_c=1$ (i.e., one atom/molecule per unit cell) there are three branches of acoustic phonons (one longitudinal and two transverse) and therefore $\eta=3$. If, instead, $N_c=2$, there are the original three acoustical branches plus three optical branches and therefore only half of the $3N$ degrees of freedom contribute to the acoustical phonon spectrum, i.e., $\eta=3/2$. For a non-spherical molecule, there are a total of $6N$ degrees of freedom which for $N_c=2$ separate into three acoustical branches and nine optical branches. The acoustical phonon spectrum represents one-fourth of the available modes and therefore $\eta=6/4=3/2$, as for example in the case of pentacene. More generally, it can be shown that $\eta=3/N_c$.

With Eq. (A7) and the following substitution of the radial variable of integration q ,

$$y = \frac{a}{(2\pi^2 \eta N_c)^{1/3}} q = \frac{v_s}{\omega_D} q, \quad (A8)$$

$$dy = \frac{v_s}{\omega_D} dq,$$

Eq. (A1) can be expressed as function of the relative energy $x = \varepsilon_k/B$ of the carrier inside the band. The result has been written in Eqs. (11)–(15).

2. Optical scattering rate

For the optical phonon scattering rate the calculation proceeds along the same line of the acoustic case, but with the phonon energy written as $\hbar\omega_0$. Considering, for simplicity, a dispersionless optical phonon, Eq. (7) for the optical case is transformed into¹

$$\frac{1}{\tau_{op}} = \frac{1}{\hbar(2\pi)^2} \int_{q_{\min}}^{q_{\max}} q^2 dq \int_0^{2\pi} d\phi \frac{g_0^2 \hbar \omega_0 a^3}{N_c \hbar \omega_0} \times [I_{op}(\vec{k} + \vec{q}) n_{q,op} + I_{op}(\vec{k} - \vec{q}) (n_{q,op} + 1)], \quad (A9)$$

where q_{\min} and q_{\max} simply indicates that the scattering rate is nonzero only for certain values of phonon momentum defined by the two following positive quantities:

$$I_{op}(\vec{k} + \vec{q}) = \int_0^\pi \delta \left[\frac{a^2 B}{(3\pi^2 N_c)^{2/3}} (q^2 + 2kq \cos \theta) - \hbar \omega_0 \right] \times \Theta \left[B - \frac{a^2 B}{(3\pi^2 N_c)^{2/3}} (q^2 + 2kq \cos \theta + k^2) \right] \sin \theta d\theta \quad (A10)$$

$$I_{op}(\vec{k} - \vec{q}) = \int_0^{\arccos \zeta} \delta \left[\frac{a^2 B}{(3\pi^2 N_c)^{2/3}} (q^2 - 2kq \cos \theta) + \hbar \omega_0 \right] \times \Theta \left[\frac{a^2 B}{(3\pi^2 N_c)^{2/3}} (q^2 - 2kq \cos \theta + k^2) \right] \sin \theta d\theta. \quad (A11)$$

As for the acoustic case, imposing the condition $q \geq 0$ on the expression in Eq. (8), corresponding to the emission process, gives a maximum angle¹² $\zeta = \sqrt{\hbar \omega_0/B}$. Again, $\zeta > 0$ implies that only forward emission is allowed and the presence of the Heaviside function Θ assures that the final momentum state of the carrier stays inside the band.

With the substitutions

$$x_{\pm} = \frac{a^2 B}{(3\pi^2 N_c)^{2/3}} (q^2 \pm 2kq \cos \theta) \mp \hbar \omega_0$$

$$dx_{\pm} = \mp \frac{a^2 B}{(3\pi^2 N_c)^{2/3}} 2kq \sin \theta d\theta \quad (A12)$$

Eqs. (A10) and (A11) become, respectively,

$$I_{op}(\vec{k} + \vec{q}) = \frac{(3\pi^2 N_c)^{2/3}}{2a^2 B k q} \int_{\hat{a}_1}^{\hat{a}_0} dx_+ \delta(x_+) \times \Theta [B - (x_+ + \varepsilon_k + \hbar \omega_0)] = \frac{(3\pi^2 N_c)^{2/3}}{2a^2 B k q} \{ [\Theta(q - k \sqrt{1 + \hbar \omega_0/\varepsilon_k} + k) - \Theta(q - k \sqrt{1 + \hbar \omega_0/\varepsilon_k} - k)] \Theta(B - \varepsilon_k - \hbar \omega_0) \}, \quad (A13)$$

$$I_{op}(\vec{k} - \vec{q}) = \frac{(3\pi^2 N_c)^{2/3}}{2a^2 B k q} \int_{\hat{e}_1}^{\hat{e}_0} dx_- \delta(x_-) \Theta[x_- + \varepsilon_k - \hbar \omega_0] = \frac{(3\pi^2 N_c)^{2/3}}{2a^2 B k q} \Theta(\varepsilon_k - \hbar \omega_0) \{ 1 - \Theta[(q - k - k \sqrt{1 - \hbar \omega_0/\varepsilon_k})(q - k + k \sqrt{1 - \hbar \omega_0/\varepsilon_k})] \}, \quad (A14)$$

where now $\hat{a}_0 = a^2 B (3\pi^2 N_c)^{-2/3} (q^2 + 2kq) - \hbar \omega_0$, $\hat{a}_1 = a^2 B (3\pi^2 N_c)^{-2/3} (q^2 - 2kq) - \hbar \omega_0$,

$$\hat{e}_0 = a^2 B (3\pi^2 N_c)^{-2/3} \left(q - \frac{(3\pi^2 N_c)^{1/3}}{a} \sqrt{\frac{\hbar \omega_0}{B}} \right)^2,$$

and $\hat{e}_1 = a^2 B (3\pi^2 N_c) (q^2 - 2kq) + \hbar \omega_0$. Equation (A9) can be integrated in q and the result can be written as function of the relative energy $x = \varepsilon_k/B$ of the carrier inside the band, as displayed in Eqs. (16)–(18).

- ¹E.M. Conwell, *High Field Transport in Semiconductors* (Academic Press, New York, 1967).
- ²J.M. Ziman, *Electrons and Phonons* (Clarendon, Oxford, 1982).
- ³R. Silbey and R.W. Munn, *J. Chem. Phys.* **72**, 2763 (1980).
- ⁴V.M. Kenkre, J.D. Andersen, D.H. Dunlap, and C.B. Duke, *Phys. Rev. Lett.* **62**, 1165 (1989).
- ⁵P. Reineker, V.M. Kenkre, and R. Kühne, *Phys. Lett. A* **84**, 294 (1981).
- ⁶See, for a review, M. Pope and C.E. Swenberg, *Electronic Processes in Organic Crystals and Polymers* (New York, Oxford, 1999).
- ⁷V.M. Kenkre, *Phys. Lett. A* **305**, 443 (2002).
- ⁸We neglect umklapp processes for simplicity.
- ⁹If regimes of very low B values (such that $\hbar\omega_D/B > 2(2\eta/3)^{1/3}$) are attained, then Umklapp processes as well as other second-order processes become important.
- ¹⁰C. Erginsoy, *Phys. Rev.* **79**, 1013 (1950).
- ¹¹A. Matthiessen, *Ann. Phys. Chem.* **110**, 190 (1860); also see A.H. Wilson, *The Theory of Metals* (Cambridge University Press, Cambridge, 1958) for a recent reference.
- ¹²B.K. Ridley, *Quantum Processes in Semiconductors* (Clarendon, Oxford, 1999).
- ¹³The high-temperature behavior of μ appears from our numerical computations to be of the form $T^{-2.5}$.
- ¹⁴Any other optical phonon scattering event would move a carrier in a region where $\rho(\varepsilon_k)=0$ and therefore is forbidden.
- ¹⁵For the case depicted in Figs. 2 and 3 we have computed the mean free path and found it to be larger than a lattice constant. However, even if extraneous scattering does not mask the predicted dip and rise, the analysis might be inapplicable to a specific system if the mean free path is of the order of, or falls below, the lattice constant. The entire Boltzmann analysis in k space, and, consequently, the predicted effect, would then be inapplicable.
- ¹⁶J.D. Andersen, C.B. Duke, and V.M. Kenkre, *Phys. Rev. Lett.* **51**, 2202 (1983).
- ¹⁷The turnover in μ reported in pentacene at higher temperature (about 400 K) requires a combination of a polaronic analysis with the present band treatment as outlined in Ref. 7.
- ¹⁸A. Brillante, R.G. Della Valle, L. Farina, A. Girlando, M. Masino, and E. Venuti, *Chem. Phys. Lett.* **357**, 32 (2002).
- ¹⁹W. Warta and N. Karl, *Phys. Rev. B* **32**, 1172 (1985).
- ²⁰J. Cornil, J.Ph. Calbert, and J.L. Bredas, *J. Am. Chem. Soc.* **123**, 1250 (1001); J.L. Bredas, D. Beljonne, J. Cornil, J.Ph. Calbert, Z. Shuai, and R. Silbey, *Synth. Met.* **125**, 107 (2002).
- ²¹There are serious concerns about the experimental support lent to bandwidth values by velocity saturation experiments. For a discussion see V.M. Kenkre and P.E. Parris, *Phys. Rev. B* **65**, 205104 (2002); **65**, 245106 (2002).
- ²²V.M. Kenkre, P. Parris, L. Giuggioli, and J.D. Andersen (unpublished).